EPTT 2018
XI Escola de Primavera de Transição e Turbulência

ABCM
Associação Brasileira de Engenharia e Ciências Mecânicas

11th Spring School on Transition and Turbulence
September 17th-21st, 2018, Uberlândia, MG, Brazil

EPTT-2018-0014
ON CLOSED-SECTION WIND-TUNNEL AEROACOUSTIC EXPERIMENTS WITH 2D HIGH-LIFT MODELS

Filipe Ramos do Amaral
University of Sao Paulo (USP), Sao Carlos School of Engineering, 13566-590, Sao Carlos, Brazil
framaral@usp.br
Carlos do Carmo Pagani Junior
Sao Paulo State University (UNESP), 13876-750, Sao Joao da Boa Vista, Brazil
carlos.pagani@sjbv.unesp.br
Fernando Henrique Tadashi Himeno
University of Sao Paulo (USP), Sao Carlos School of Engineering, 13566-590, Sao Carlos, Brazil
fernando.himeno@usp.br
Daniel Sampaio Souza
Federal University of Sao Joao del-Rei (UFSJ), 36307-352, Sao Joao del-Rei, Brazil
dss-em@usp.br
Matheus Maia Beraldo
University of Sao Paulo (USP), Sao Carlos School of Engineering, 13566-590, Sao Carlos, Brazil
matheusberaldo@usp.br
Marcello Augusto Faraco de Medeiros
University of Sao Paulo (USP), Sao Carlos School of Engineering, 13566-590, Sao Carlos, Brazil
marcello@sc.usp.br

Abstract. *Two-dimensional high-lift airfoil models noise investigations are normally conducted in closed-section wind-tunnels owing to their convenience in comparison to open-section ones for aerodynamic measurements, although many difficulties arise in aeroacoustic tests at closed-section tunnels. The interaction between the test-section wall boundary-layers and the model ends leads to three-dimensional effects, which impact the model lift, hence, the noise emission. Reverberation and acoustic images can also interfere with the measurements. This paper addresses the effects of the aforementioned issues on MD30P30N airfoil slat aeroacoustic measurements. Conventional beamforming was employed for the acoustic data post-processing and pressure taps were used in the high-lift airfoil model spanwise and chordwise pressure coefficients assessment. Wind-tunnel side-wall boundary-layer suction was applied, rendering a more two-dimensional flow and correcting the model angle of attack by approximately 2 deg. Acoustic melamine -based foam was applied on the test-section walls for reducing reverberation effects on the interpretation of slat noise source maps, although the effects of the source images on both the noise source maps and noise spectra in the region of interest were considered small. The CW phased array shading scheme effect on the source two-dimensionality was also assessed, and it was verified it enhanced the slat noise source two-dimensional character.*

Keywords: *closed-section wind-tunnels, boundary-layer side-wall suction, acoustic treatment, conventional beamforming, aeroacoustics*

1. INTRODUCTION

Aeroacoustic measurements of high-lift models benefit from the well-defined boundary conditions of closed-section wind-tunnels, which reduce uncertainties in the flow incidence angle and facilitate the establishment of boundary conditions for corresponding numerical simulations. Nevertheless, the incoming flow is generally not uniform owing to the development of relatively thick boundary-layers along the wind-tunnel walls. The flow three-dimensionality, more pronounced for lifting models, promotes flow variations along the model span and reduces the model lift, which may be interpreted as an effective reduction of the model's angle of attack (Paschal *et al.*, 1991). Several techniques aim at avoiding the three-dimensionality effects; they constitute some type of boundary-layer controls of which the most common ones are tangential blowing and suction (Paschal *et al.*, 1991; Catalano and Caixeta, 2004; Pascioni *et al.*, 2014) and lead to a more uniform flow distribution over the model

span.

In closed-section wind-tunnels, mirror sources may interfere with real sources (Sijtsma and Holthusen, 2003; Fleury and Davy, 2012; Fleury *et al.*, 2015). Soderman *et al.* (2002); Syms (2012) studied the effect of the use of foam on the wind-tunnel test-section walls for reverberation control and other approaches were considered by Smith *et al.* (2005) and Ito *et al.* (2010). Reverberation control is certainly wind-tunnel-dependent and more data are necessary for the establishment of best practices.

This study investigates the application of side-wall boundary-layer suction for two-dimensional lifting bodies experiments. Closed-section wind-tunnel acoustic reverberation was also assessed through tests performed with the working section subject to an acoustic treatment and compared with the untreated one. MD30P30N high-lift airfoil model (Valarezo *et al.*, 1991; Chin *et al.*, 1993) was the lifting body employed for the experiments and its slat noise (Choudhari *et al.*, 2002; Guo *et al.*, 2003; Dobrzynski, 2010; Pagani *et al.*, 2016, 2017) was the studied case. Conventional beamforming in-house codes (Amaral *et al.*, 2015; Pagani *et al.*, 2016, 2017; Amaral *et al.*, 2018a) implemented in the frequency domain, were employed for the acoustic measurements, whereas airfoil surface pressure tappings enabled the measurement of chordwise and spanwise static pressure coefficient distributions. The CW array shading scheme, introduced by Amaral *et al.* (2018a), was applied over the foamed-walls experiments in order to investigate its effect on the two-dimensional slat source representation.

2. METHODOLOGY

The two-dimensional three-element MD30P30N high-lift airfoil test model has 1,300 mm span and 500 mm stowed chord and is basically manufactured in aluminum alloy (Amaral *et al.*, 2015; Pagani *et al.*, 2016, 2017; Amaral *et al.*, 2018a). The MD30P30N slat chord is 15% and its gap and overlap are 2.95% and -2.50%, respectively, whereas the chord of the flap is 30% and its gap and overlap are 1.27% and 0.25%, respectively. Percentages are referenced to the airfoil stowed chord. 143 pressure tappings in the middle span, along a chordwise line, and 40 pressure tappings distributed along the span at two positions on the suction side, near the main element leading and trailing edges, assessed the pressure distribution over the model.

The experiments were conducted in a low-speed closed-circuit single return wind-tunnel (Santana *et al.*, 2014) of 1.3 m high, 1.7 m wide and 3 m long closed-section. The high-lift model was vertically mounted and spanned the entire test-section height and the model ends were attached to lower and upper circular turntables, the former coupled to a mechanism for enabling adjustments in the airfoil angle of attack. Aeroacoustic experiments were conducted for the test-section with hard- (Fig. 1a) and foamed- walls (Figs. 1b and 1c). The acoustic treatment used to control acoustic reverberation consisted in the application of a coating of 25 mm thick melamine foam installed on the top, bottom and model suction side test-section walls. The foam was not flush-mounted for avoiding severe modifications in the experimental setup, nevertheless, its edges were wedge-shaped.

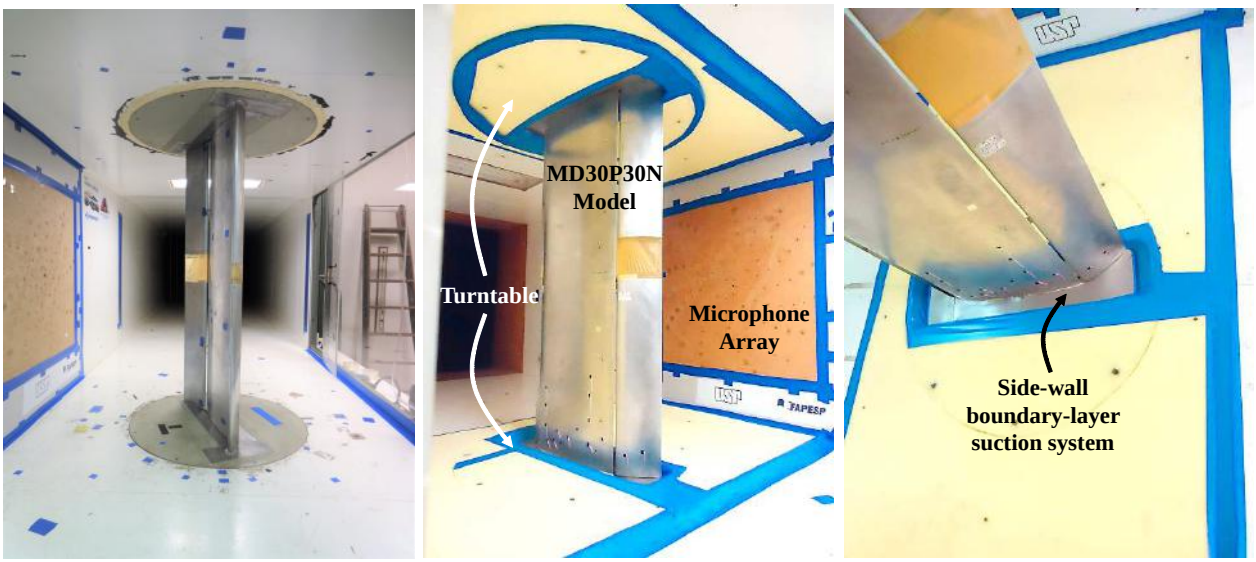

(a) Hard-walls configuration (b) Foamed-walls configuration (c) Detail on the suction porous plate

Figure 1: Wind-tunnel test-section and airfoil model in the hard- and foamed- walls configurations.

The facility supported wind-tunnel wall boundary-layer suction applied through a stainless steel porous plate around the model's main element suction side and the slat leading edge, Fig. 1c. The suction level was controlled by an external centrifugal fan connected to the wind-tunnel test-section top and bottom walls through two hoses.

Wall boundary-layer suction was also applied in the foamed setup, as the foam was removed near the model/walls juncture, Fig. 1c. Measurements were performed for 34 m/s freestream speed (0.1 Mach number and 9.62×10^5 Reynolds number based on the model stowed chord). The angles of attack were set between 2 deg and 8 deg.

A 62 flush-mounted microphone array of 850 mm aperture microphone array (Fonseca *et al.*, 2010) was employed for the aeroacoustic measurements, mounted on the wind-tunnel test-section lateral wall, facing the high-lift pressure side. Conventional beamforming (Mueller *et al.*, 2002) in-house codes (Amaral *et al.*, 2015; Pagani *et al.*, 2016, 2017; Amaral *et al.*, 2018a,b) were implemented in the frequency domain and used for the acoustic data post-processing. The acoustic signals were acquired during 39 s at a 51.2 kHz sample rate. Frequencies were divided into narrowbands of different resolutions along the frequency range of interest, therefore, different lengths of data blocks were employed, Tab. 1.

Table 1: Discretization of the narrowband frequencies employed for Power Spectral Density estimations.

Frequency Range, kHz	Frequency Resolution, Hz	Number of blocks
0.50-1.60	25	1947
1.65-3.20	50	3895
3.30-6.40	100	7791
6.60-12.80	200	15584
13.20-25.20	400	31170

Figure 2 shows the spatial mesh applied for the calculation of the beamforming maps, which was defined in a rectangular domain (dotted lines) of 1,400 mm and 300 mm minimum dimensions in spanwise and streamwise directions, respectively, centered at the slat mid-span and mid-chord, 850 mm from the array plane. For the acoustic treatment effect assessment, the mesh spanwise minimum dimension was 4,000 mm. The region of interest (ROI), i.e., the mesh sub-domain defined for the evaluation of the slat noise spectra from the array measurements (dashed lines), was centered in the domain and measured 800 mm and 180 mm in the spanwise and streamwise directions, respectively, Fig. 2a. Two other ROIs, near the junction between the slat model and the test-section top and bottom walls, were also employed for the assessment of the sound produced by the suction system and the junction and measured 200 mm and 180 mm in the spanwise and streamwise directions, respectively, Fig. 2a. Moreover, in order to verify the slat acoustic source two-dimensionality, the model spanwise direction was divided into 13 subsequent sectors of 100 mm spanwise and 180 mm streamwise dimensions, Fig. 2b, and for each ROI sector, the correspondent noise spectra were computed.

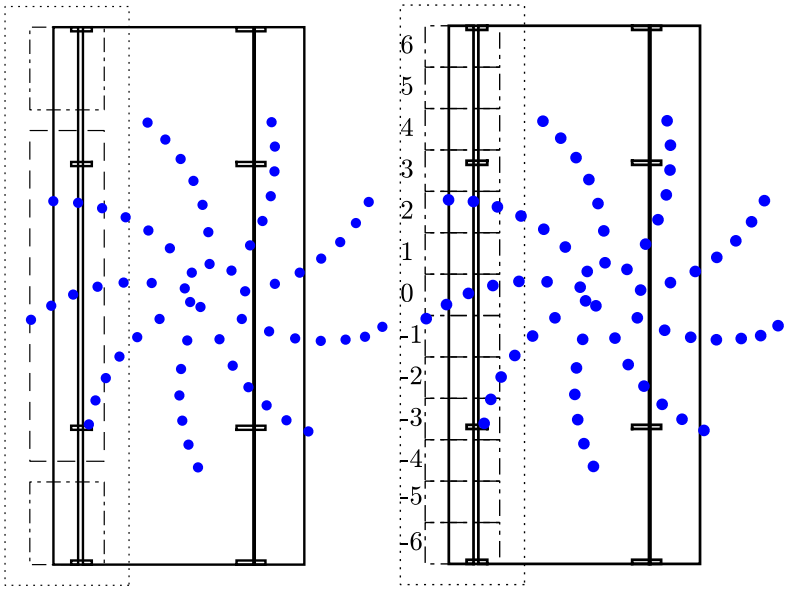

(a) Central, top and bottom ROIs (b) 13 sectors ROIs

Figure 2: Diagram containing the projection of the airfoil model (continuous lines) on the array (filled circles), the spatial mesh (dotted lines) and the ROIs (dashed lines). The flow is directed from left to right.

3. RESULTS

3.1 Wind-tunnel side-wall boundary-layer control

Figure 3 shows chordwise pressure coefficient (c_p) distributions in the model middle span and spanwise c_p distributions at two chordwise positions, near the leading (top curves) and trailing edges (bottom curves) of the airfoil model main element, respectively. The test cases corresponded to 2 and 8 deg angles of attack (AOA) with different levels of boundary-layer suction applied. Table 2 shows the suction pump flow rate as percentages relative to the closed-section flow rate at 34 m/s freestream speed.

Table 2: Wind-tunnel side-wall boundary-layer suction levels.

Suction level	2 deg AOA	8 deg AOA
0	0%	0%
1	0.01%	0.01%
2	0.02%	0.02%
3	-	0.05%
4	-	0.07%

An increase in the suction level provided a more uniform spanwise c_p distribution along the span. This effect is clearer at 8 deg AOA, as the higher the model lift, the higher the flow three-dimensionality and the higher the suction required for spanwise uniformity. At 8 deg AOA, a substantial three-dimensionality reduction was achieved by the setting of suction at level 3, whereas only a small improvement was obtained by the increase in the suction from level 3 to 4, Fig. 3c. Therefore, level 3 was regarded as a good level for an effective boundary-layer control, beyond which only a marginal improvement in the flow uniformity would be achieved at the risk of over suction. At 2 deg AOA, the suction impact on the chordwise distribution was very small and level 2 was regarded as a good level for an effective boundary-layer control. Steady-state, two-dimensional OpenFOAM simulations were employed for obtaining the mean flow around the airfoil and details on mesh, domain and flow parameters are provided by Amaral *et al.* (2018a). The numerical chordwise c_p data are also displayed in Fig. 3 and generally showed a better agreement with the experimental results for the main element when boundary-layer suction was applied.

Figure 4 shows conventional beamforming noise spectra for 0 to 3 suction rates. The results clearly indicate the suction effect. At 2 deg AOA, the suction rate is small and its effect is almost insignificant, whereas at 8 deg AOA angle of attack, the suction substantially reduced the slat noise intensity level, i.e., more than 3 dB for suction level 4 at certain noise spectrum features, such as low-frequency narrowband peaks and high-frequency hump. The high-frequency hump component was also shifted toward higher frequencies, as the suction level increased. All effects exerted by the suction on the noise spectra were consistent with an increase in the model angle of attack (Pagani *et al.*, 2016; Paschal *et al.*, 1991) of approximately 2 deg for 8 deg AOA and between 1 and 2 deg for 2 deg AOA.

Comparisons of noise signatures at three distinct ROIs were performed - one centered at the slat mid-span, i.e., the one employed for the slat noise evaluation (the center ROI), and two others, near the junction between the slat model and the wind-tunnel ceiling and floor walls, employed for the evaluation of the noise produced by the model/wall junction and the suction system, i.e., the top and bottom ROIs, Fig. 2a. Figure 5 shows conventional beamforming noise spectra Power Spectral Density (PSD) for the three ROIs depicted in Fig. 2a, at 2 and 8 deg AOAs, for cases with an optimal suction level applied ($w/$) and with no suction (w/o). The spectra from the central ROI show the characteristic spectral components of the slat noise, namely, low-frequency narrowband peaks, mid-frequency broadband and high-frequency hump (Choudhari *et al.*, 2002; Guo *et al.*, 2003; Dobrzynski, 2010; Souza *et al.*, 2013, 2015; Himeno *et al.*, 2016, 2017a,b). On the other hand, the spectra from the end ROIs are generally below the level attained by the central ROI, which indicates that the model end effects and suction do not produce important spurious noise in the frequency range of interest. Note two peaks at 5.2 and 7 kHz emerge from the 2 deg AOA spectra without suction - such peaks will be further investigated with the following noise source maps.

Figure 6 shows conventional beamforming noise source maps for selected frequencies at 2 and 8 deg angles of attack. The three ROIs, Fig. 2a, are indicated in dashed rectangles and airfoil element projections on the microphone array wall and the brackets employed for their positioning are also provided. Frames 6a-6d show noise source maps at frequencies corresponding to the slat noise second low-frequency narrowband peak, 1.175 kHz, and the tonal peak which emerged at 5.2 kHz for the model at 2 deg angle of attack without suction. The slat noise spectral signature was only slightly modified by the optimal suction applied to the model at 2 deg angle of attack and the noise source maps were similar for cases with and without suction, although a small increase of

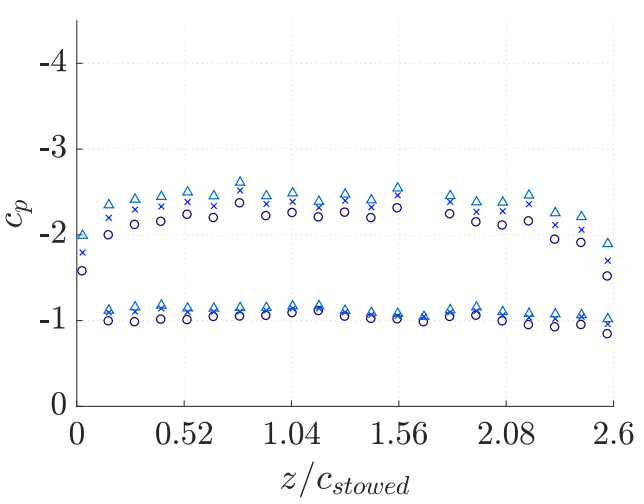

(a) 2 deg AOA, spanwise c_p

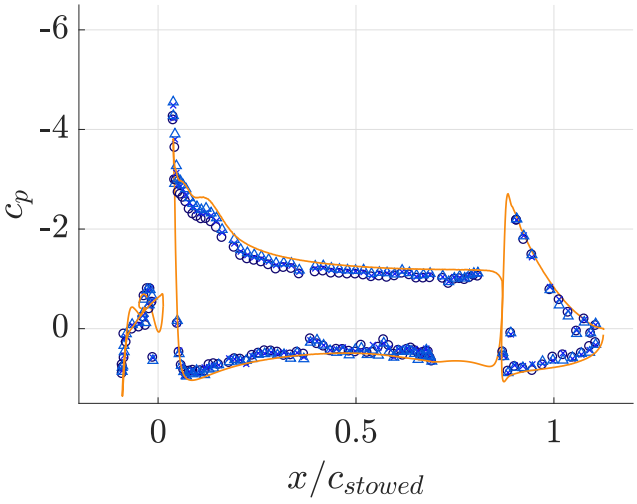

(b) 2 deg AOA, chordwise c_p

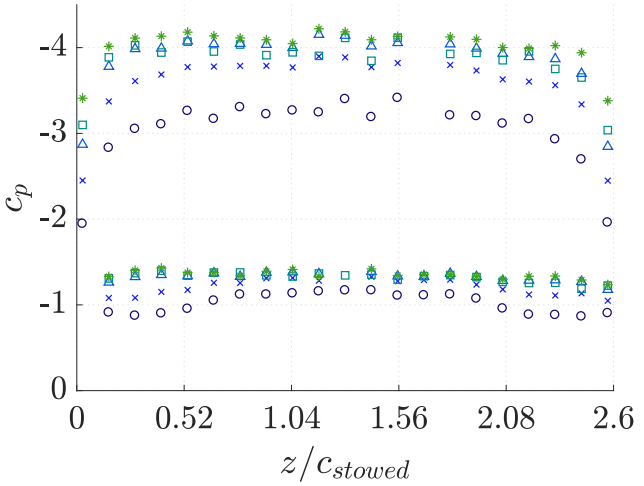

(c) 8 deg AOA, spanwise c_p

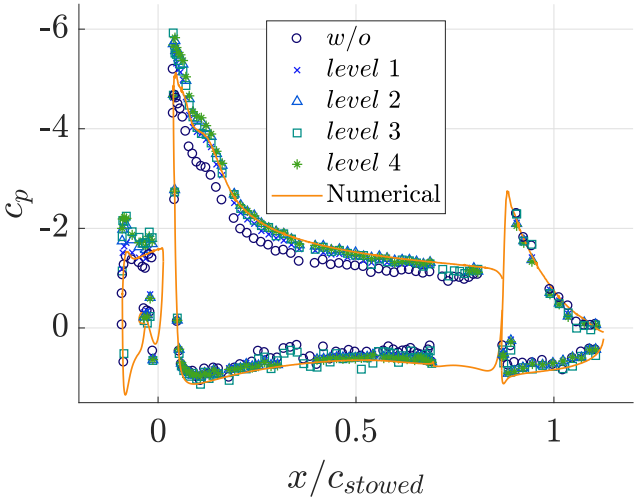

(d) 8 deg AOA, chordwise c_p

Figure 3: Pressure coefficient distribution along chordwise and spanwise directions for several suction rates.

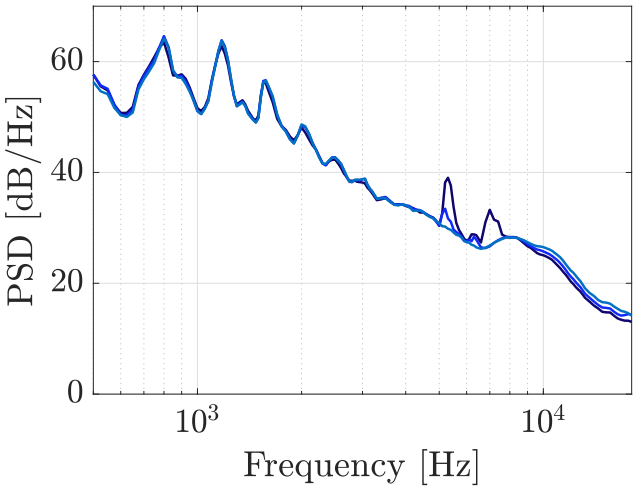

(a) 2 deg AOA

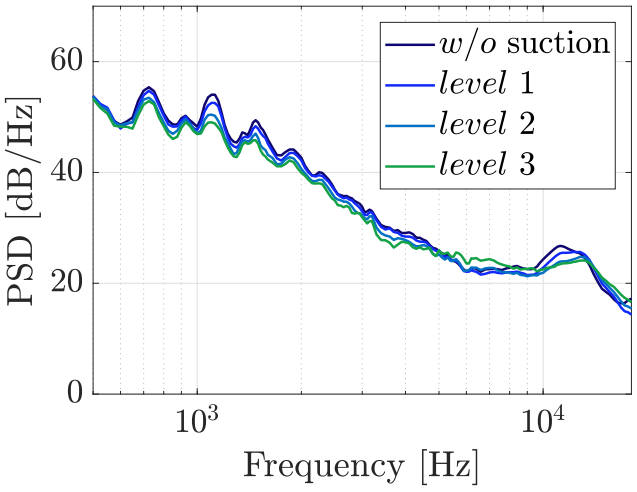

(b) 8 deg AOA

Figure 4: Conventional Beamforming slat noise spectra for several suction rates.

approximately 1 dB/Hz in the noise levels for the low-frequency narrowband peak component was observed after the application of suction. At 5.2 kHz frequency, the bottom ROI shows a strong source on the conventional beamforming map, Figs. 6c and 6d, an a peak emerge from the noise spectra and no suction configuration, Fig.

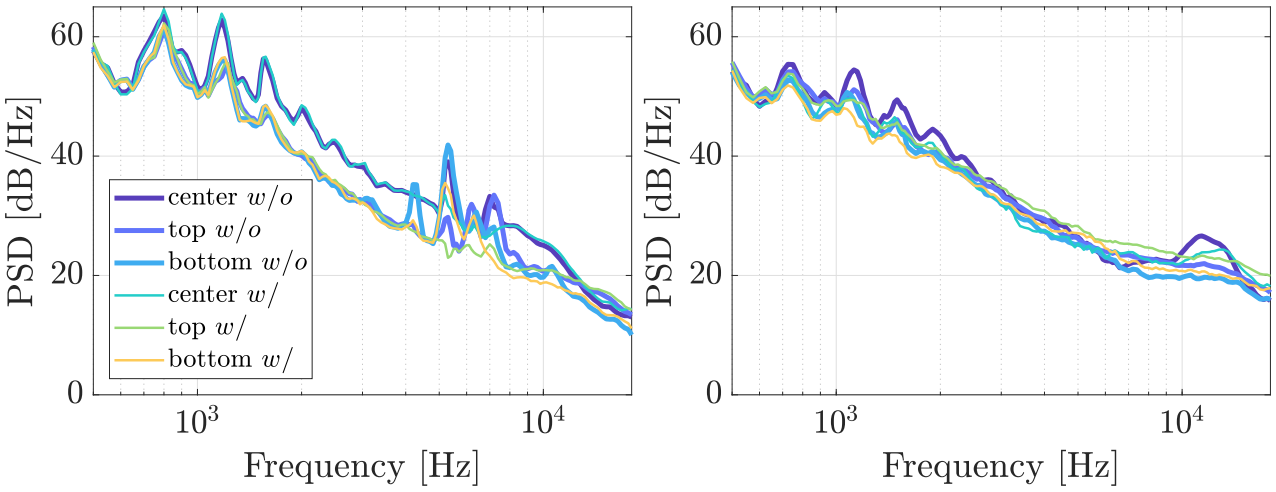

(a) 2 deg AOA (b) 8 deg AOA

Figure 5: Conventional beamforming slat noise spectra for the three ROIs of Fig. 2a and cases with and without suction.

4a. The noise source map shows a strong source of approximately a 41 dB/Hz peak level when no suction was applied, whereas after the application of suction, such level was reduced by approximately 5 dB/Hz, which could explain the noise spectrum peak suppression observed after the application of suction, Fig. 4a.

The suction is not associated with the model ends sources and, rather, reduces its level. The results do not show strong sources associated with the brackets Pagani *et al.* (2016). Frames 6e-6h display noise source maps at frequencies corresponding to the slat noise third low-frequency narrowband peak, 1.5 kHz, and the broadband component at 7 kHz, i.e., a frequency at which the noise spectra of the model/wall junction ROI showed higher intensity levels than the central ROI for the model at 8 deg angle of attack, Fig. 5b. At lower frequencies, the conventional beamforming noise source map provides a wide source whose peaks are located outside the central ROI. At 7 kHz, the conventional beamforming noise source map shows dominant sources located at the end ROIs, which are slightly enhanced by suction and, as a consequence, the sources in the central ROI are not contaminated.

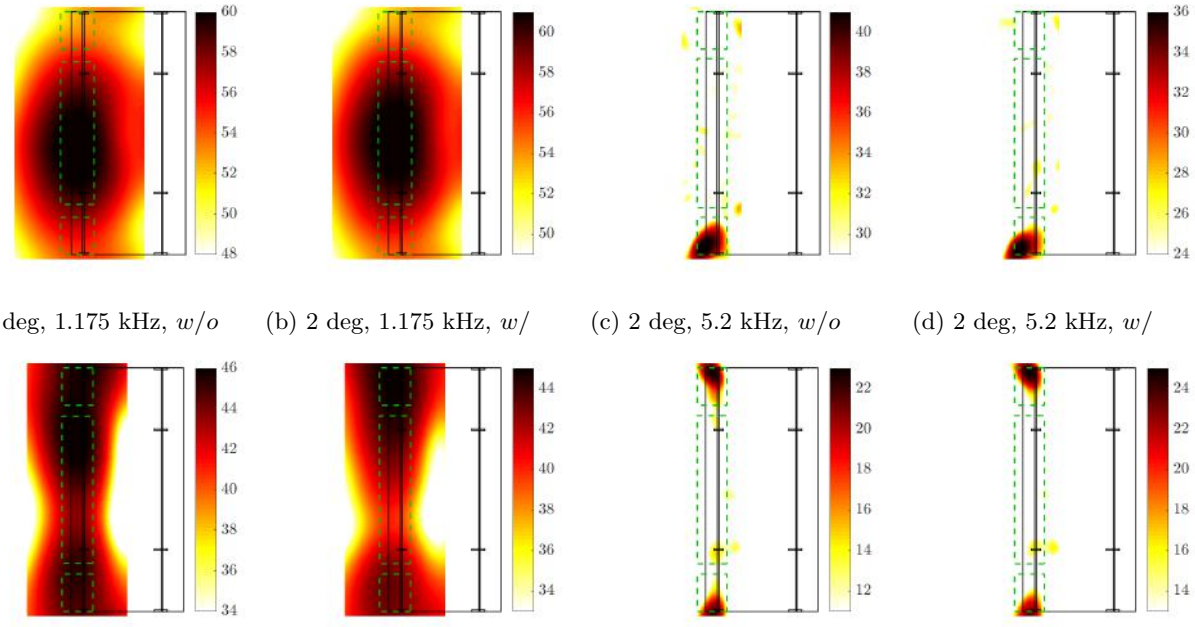

(a) 2 deg, 1.175 kHz, w/o (b) 2 deg, 1.175 kHz, $w/$ (c) 2 deg, 5.2 kHz, w/o (d) 2 deg, 5.2 kHz, $w/$

(e) 8 deg, 1.5 kHz, w/o (f) 8 deg, 1.5 kHz, $w/$ (g) 8 deg, 7 kHz, w/o (h) 8 deg, 7 kHz $w/$

Figure 6: Slat noise source maps for cases with optimal suction applied ($w/$) and without suction (w/o).

3.2 Acoustic treatment on the test-section walls

Acoustic measurements were conducted for the foamed-walls experimental setup, Fig. 1b, for the evaluation of the effect of source images associated with the working section wall. Note boundary-layer suction was also applied to this setup, Fig. 1c. For the foamed-walls experiment, the model was set at 4 deg AOA. Conventional beamforming noise source maps are shown in Fig. 7 for a frequency corresponding to a slat noise spectra narrowband peak (1.15 kHz), a valley (1.9 kHz), the broadband region (4.4 kHz) and the high-frequency hump (10.8 kHz), Fig. 8. The source of the setup with no acoustic treatment extends well beyond the test-section and the acoustic treatment drastically reduced the image magnitudes, while, within the test–section, the source conformed slightly more closely to a line.

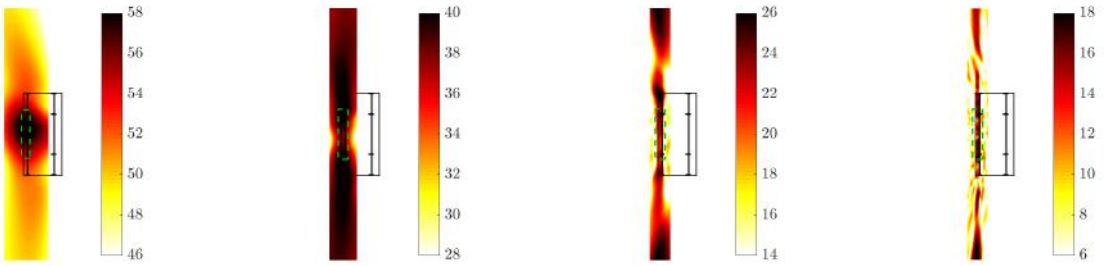

(a) 1.15 Hz (hard-walls) (b) 1.9 kHz (hard-walls) (c) 4.4 kHz (hard-walls) (d) 10.8 kHz (hard-walls)

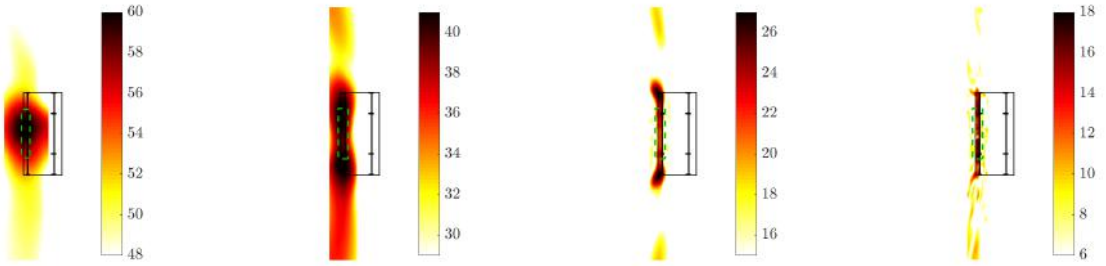

(e) 1.15 kHz (foamed-walls) (f) 1.9 kHz (foamed-walls) (g) 4.4 kHz (foamed-walls) (h) 10.8 kHz (foamed-walls)

Figure 7: Conventional beamforming slat noise source maps at selected frequencies for experimental setups with hard- (frames 7a-7d) and foamed- (frames 7f-7h) walls for 4 deg AOA.

Figure 8 shows a comparison of slat noise spectra measured in the wind-tunnel test-section with foamed- and hard-walls integrated in the central ROI previously described. The CW scheme was also tested over the foamed-walls results. The spectra with and without foam agreed well throughout the frequency range of interest, although an approximately 3 dB/Hz increase was observed in the level of the two first narrow-band peaks when foamed-walls set up. As the beamforming maps obtained with acoustic treatment are more reliable, the sound level estimates are likely to be more accurate. Nevertheless, for most circumstances, the acoustic treatment may be considered unnecessary. For hard-wall closed-section wind-tunnel practice, with an appropriate ROI, the results from conventional beamforming can provide reliable spectral estimates. As expected, the use of CW array shading scheme (Amaral *et al.*, 2018a) provided higher spectral estimates, especially from mid to high frequencies, for which a 3 dB/Hz spectral level increase was observed. Such noise spectra estimates seems to be more reliable, since the CW scheme over-weights the array microphones signals which remain more coherent with the other ones for each frequency of interest.

Figure 9 exhibits a study on the slat source two-dimensionality, for which the noise spectra were evaluated for the 13 ROI sectors previously defined in Fig. 2b. The dashed lines indicate the central ROI spanwise dimension, i.e., 800 mm between sectors -4 and 4. The study was conducted with the test-section in the hard- and foamed-walls configurations and the CW array shading scheme was tested only in the foamed-walls set up.

The results exhibit an excellent two-dimensional pattern, mainly between -4 to 4 sectors, i.e., the central ROI 800 mm spanwise extent. Sectors near the test-section walls, i.e., 5, 6, -5 and -6, show lower levels of spectral content when hard-wall set up, which is more pronounced for higher frequencies. The application of foam coating over the test-section walls enhanced the noise source spectra two-dimensionality over the 13 sectors, mainly in the slat noise spectra low-frequency narrowband peaks (0.775, 1.15 and 1.525 kHz), and in the valley between 4 and 8 kHz frequencies, Fig. 9b. Moreover, the combination of the CW array shading scheme and foamed-walls

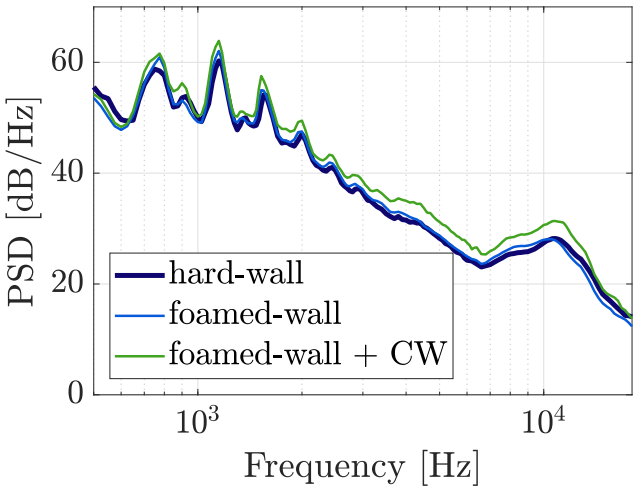

Figure 8: Conventional beamforming slat noise spectra obtained from acoustic measurements for the test-section setup with foamed and hard walls.

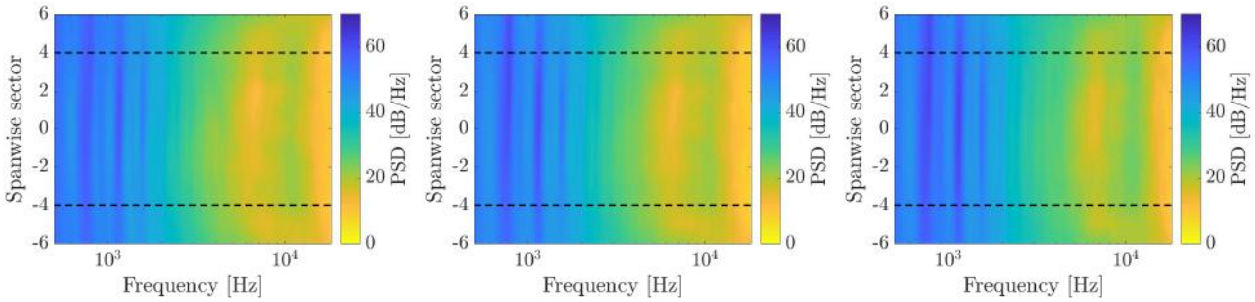

(a) CBF, Hard-wall (b) CBF, Foamed-wall (c) CBF-CW, Foamed-wall

Figure 9: Slat noise spectra contour plots for the 13 ROI spanwise sectors.

set up provided an even more two-dimensional slat noise spectra distribution over the 13 ROIs, mainly in in the valley between 4 and 8 kHz frequencies and the high frequency hump (around 10.6 kHz), Fig. 9c. The CW scheme was more effective in the mid- to high- frequencies, as the spectra showed higher intensity levels and uniformity over the model span, whereas the foamed-walls enhanced the noise source two-dimensionality character in the low-frequency ranges, mainly over the low-frequency narrowband peaks slat components

4. CONCLUSION

This study investigated procedures applied to improve the quality of aeroacoustic experiments of two-dimensional high-lift airfoils in a closed-section wind-tunnel. Wind-tunnel test-section wall boundary-layer suction was an effective approach for reducing flow three-dimensionalities along the model span. Consistently with previous aerodynamic studies, in the current setup, the lack of boundary-layer control led to errors that may correspond to a 2 deg AOA variation. In general, the model end effects and suction did not constitute strong noise sources and where the noise from the slat shows low intensity levels, the sources associated with model ends and suction were restricted to the neighborhood of the test-section walls. The use of a ROI that excluded a small region close to the walls was enough to avoid contamination from those undesirable effects. Wind-tunnel side-wall boundary-layer control via suction was considered both important, as it corrects the model effective angle of attack, and viable, as it did not introduced any spurious noise to the noise spectra estimations. Test-section hard-walls produced acoustic images throughout the frequency range of interest. The application of an acoustic treatment on the walls reduced the magnitude of such images and enhanced source representation, although the foam effect on a ROI that avoided regions close to the walls was very small on both noise source maps and spectra. Regarding the slat noise source spectrum two-dimensionality, the combination of foamed-walls with the CW array shading scheme provided the best results, improving the spectral levels and two-dimensionality over the entire frequency range of interest. Acoustic treatment in closed-section wind-tunnels for experiments with two-dimensional lifting bodies is unnecessary, once even conventional beamforming produced good estimates for an appropriate ROI.

5. ACKNOWLEDGEMENTS

F.R.A. and D.S.S. received funding from Coordination for the Improvement of Higher Education Personnel (CAPES/Brazil - grant #00011/07-0). C.C.P. received support from Sao Paulo Research Foundation (FAPESP/Brazil) and EMBRAER/Brazil in the Brazilian Silent Aircraft Program (grant #2006/52568-7) and from National Council for Scientic and Technological Development (CNPq/Brazil - grant #141755/2012-1). F.H.T.H. received support from FAPESP/Brazil, grant #2016/02970-5. M.A.F.M. received support from CNPq/Brazil (grant #304859/2016-8). The authors acknowledges EMBRAER/Brazil for the many fruitful contributions and Marlon Sproesser Mathias for his technical support.

6. REFERENCES

Amaral, F.R., Himeno, F.H.T., Pagani, Jr, C.C. and Medeiros, M.A.F., 2018a. "Slat noise from an md30p30n airfoil at extreme angles of attack". *AIAA Journal*, Vol. 56, No. 3, pp. 964–978. ISSN 0001-1452. doi: https://doi.org/10.2514/1.J056113.

Amaral, F.R., Serran, Rico, J.C. and Medeiros, M.A.F., 2018b. "Design of microphone phased arrays for acoustic beamforming". *Journal of the Brazilian Society of Mechanical Sciences and Engineering (accepted)*. ISSN 1806-3691.

Amaral, F.R., Souza, D.S., Pagani, Jr, C.C., Himeno, F.H.T. and Medeiros, M.A.F., 2015. "Experimental study of the effect of a small 2d excrescence placed on the slat cove surface of an airfoil on its acoustic noise". In *21st AIAA/CEAS Aeroacoustics Conference*. p. 3138. doi: https://doi.org/10.2514/6.2015-3138.

Catalano, F.M. and Caixeta, Jr, P.R., 2004. "Wind tunnel wall boundary layer control for 2d high lift wing testing". In *24th International Congress of the Aeronautical Sciences*. URL `http://icas.org/ICAS_ARCHIVE/ICAS2004/PAPERS/103.PDF`.

Chin, V., Peters, D., Spaid, F. and McGhee, R., 1993. "Flowfield measurements about a multi-element airfoil at high reynolds numbers". Technical report, NASA Technical Reports. URL `https://ntrs.nasa.gov/search.jsp?R=19930064303`.

Choudhari, M.M., Lockard, D.P., Macaraeg, M.G., Singer, B.A., Streett, C.L., Neubert, G.R., Stoker, R.W., Underbrink, J.R., Berkman, M.E. and Khorrami, M.R., 2002. "Aeroacoustic experiments in the langley low-turbulence pressure tunnel". Technical report, NASA TM.

Dobrzynski, W., 2010. "Almost 40 years of airframe noise research: What did we achieve?" *Journal of Aircraft*, Vol. 47, No. 2, pp. 353–367. ISSN 0021-8669. doi: https://doi.org/10.2514/1.44457.

Fleury, V. and Davy, R., 2012. "Beamforming-based noise level measurements in hard-wall closed-section wind tunnels". In *18th AIAA/CEAS Aeroacoustics Conference (33rd AIAA Aeroacoustics Conference)*. p. 2226. doi: https://doi.org/10.2514/6.2012-2226.

Fleury, V., Bulté, J., Davy, R., Manoha, E. and Pott-Pollenske, M., 2015. "2d high-lift airfoil noise measurements in an aerodynamic wind tunnel". In *21st AIAA/CEAS Aeroacoustics Conference*. p. 2206. doi: https://doi.org/10.2514/6.2015-2206.

Fonseca, W.D., Ristow, J.P., Sanches, D.G. and Gerges, S.N.Y., 2010. "A different approach to archimedean spiral equation in the development of a high frequency array". In *SAE Technical Paper*. SAE International, p. 10. doi: https://doi.org/10.4271/2010-36-0541.

Guo, Y., Yamamoto, K. and Stoker, R., 2003. "Component-based empirical model for high-lift system noise prediction". *Journal of Aircraft*, Vol. 40, No. 5, pp. 914–922. doi: https://doi.org/10.2514/2.6867.

Himeno, F.H., Amaral, F.R. and Medeiros, M.A.F., 2017a. "Aeroacoustic effect of a seal position attached in slat cove surface". In *Proceedings of the 24th ABCM International Congress of Mechanical Engineering (COBEM2017)*. Brazilian Society of Mechanical Sciences and Engineering (ABCM).

Himeno, F.H., Amaral, F.R. and Medeiros, M.A.F., 2017b. "Linear stability theory applied in a cross-stream profile of a shear layer of a leading edge slat". In *Proceedings of the XXXVIII Iberian Latin-American Congress on Computational Methods in Engineering*. Brazilian Society of Engineering Computational Methods (ABMEC).

Himeno, F.H., Souza, D.S., Amaral, F.R. and Medeiros, M.A.F., 2016. "Computational analysis of aeroacoustic effect of a seal on slat cove for different angles of attack". In *Proceedings of the 16th Brazilian Congress of Thermal Sciences and Engineering (ENCIT2016)*. Brazilian Society of Mechanical Sciences and Engineering (ABCM).

Ito, T., Ura, H., Nakakita, K., Yokokawa, Y., Wing, F.N., Burdisso, R., Iwasaki, A., Fujita, T., Ando, N., Shimada, N. and Yamamoto, K., 2010. "Aerodynamic/aeroacoustic testing in anechoic closed test sections of low-speed wind tunnels". In *16th AIAA/CEAS Aeroacoustics Conference*. p. 3750. doi: https://doi.org/10.2514/6.2010-3750.

Mueller, T.J., Allen, C.S., Blake, W.K., Dougherty, R.P., Lynch, D., Soderman, P.T. and Underbrink, J.R., 2002.

Aeroacoustic Measurements. Springer, Berlin.

Pagani, Jr, C.C., Souza, D.S. and Medeiros, M.A.F., 2016. "Slat noise: Aeroacoustic beamforming in closed-section wind tunnel with numerical comparison". *AIAA Journal*, Vol. 54, No. 7, pp. 2100–2115. ISSN 0001-1452. doi: https://doi.org/10.2514/1.J054042.

Pagani, Jr, C.C., Souza, D.S. and Medeiros, M.A.F., 2017. "Experimental investigation on the effect of slat geometrical configurations on aerodynamic noise". *Journal of Sound and Vibration*, Vol. 394, pp. 256–279. doi: https://doi.org/10.1016/j.jsv.2017.01.013.

Paschal, K., Goodman, W., Mcghee, R., Walker, B. and Wilcox, P., 1991. "Evaluation of tunnel sidewall boundary-layer-control systems for high-lift airfoil testing". In *9th Applied Aerodynamics Conference*. Fluid Dynamics and Co-located Conferences, p. 3243. doi: https://doi.org/10.2514/6.1991-3243.

Pascioni, K., Cattafesta, L.N. and Choudhari, M.M., 2014. "An experimental investigation of the 30p30n multi-element high-lift airfoil". In *20th AIAA/CEAS Aeroacoustics Conference*. AIAA Aviation, p. 3062. doi: https://doi.org/10.2514/6.2014-3062.

Santana, L.D., Carmo, M., Catalano, F.M. and Medeiros, M.A.F., 2014. "The update of an aerodynamic wind-tunnel for aeroacoustics testing". *Journal of Aerospace Technology and Management*, Vol. 6, pp. 111 – 118. ISSN 2175-9146. doi: 10.5028/jatm.v6i2.308. URL `http://www.scielo.br/scielo.php?script=sci_arttext&pid=S2175-91462014000200111&nrm=iso`.

Sijtsma, P. and Holthusen, H., 2003. "Corrections for mirror sources in phased array processing techniques". In *9th AIAA/CEAS Aeroacoustics Conference*. p. 3196. doi: https://doi.org/10.2514/6.2003-3196.

Smith, B.S., Camargo, H.E., Burdisso, R.A. and Devenport, W.J., 2005. "Development and testing of a novel acoustic wind tunnel concept". In *11th AIAA/CEAS Aeroacoustics Conference*. p. 3053. doi: https://doi.org/10.2514/6.2005-3053.

Soderman, P.T., Jaeger, S.M., Hayes, J.A. and Allen, C.S., 2002. "Acoustic quality of the 40-by 80-foot wind tunnel test section after installation of a deep acoustic lining". Technical report, NASA Technical Reports. URL `https://ntrs.nasa.gov/search.jsp?R=20040045260`.

Souza, D.S., Rodriguez, D. and Medeiros, M.A.F., 2013. "A study of the sources of slat noise using proper orthogonal decomposition". In *19th AIAA/CEAS Aeroacoustics Conference*. p. 2163. doi: https://doi.org/10.2514/6.2013-2163.

Souza, D., Rodriguez, D., Simoes, L. and Medeiros, M., 2015. "Effect of an excrescence in the slat cove: Flow-field, acoustic radiation and coherent structures". *Aerospace Science and Technology*, Vol. 44, pp. 108–115. ISSN 1270-9638. doi: https://doi.org/10.1016/j.ast.2015.01.016.

Syms, F., 2012. "Acoustic upgrades to wind tunnels at the natoinal research council canada". In *18th AIAA/CEAS Aeroacoustics Conference (33rd AIAA Aeroacoustics Conference)*. p. 2180. doi: https://doi.org/10.2514/6.2012-2180.

Valarezo, W., Dominik, C., McGhee, R., Goodman, W. and Paschal, K., 1991. "Multi-element airfoil optimization for maximum lift at high reynolds numbers". In *9th Applied Aerodynamics Conference*. p. 3332. doi: https://doi.org/10.2514/6.1991-3332.

7. RESPONSIBILITY NOTICE

The authors are the only responsible for the printed material included in this paper.